Bonding of NO_2 to the Au Atom and Au(111) Surface: A Quantum Chemical Study

Xin Lu, Xin Xu,* Nanqin Wang, and Qianer Zhang

State Key Laboratory for Physical Chemistry of Solid Surfaces, Institute of Physical Chemistry, Department of Chemistry, Xiamen University, Xiamen 361005, China

Received: March 15, 1999; In Final Form: September 13, 1999

Adsorption of NO_2 on Au(111) surface, as well as bonding in $AuNO_2$, has been investigated by means of ab initio and density functional calculations. For the $AuNO_2$ complex, both MP2 and B3LYP calculations predict three isomers, namely *trans*-η^1-O nitrito, *cis*-η^1-O nitrito and η^1-N nitro isomers, among which the latter two isomers would have comparable stability and are candidates for the ground state of the complex. The η^2-O,O′ nitrito isomer has also been considered and was found to be a transition state. For NO_2 adsorption on Au(111), our B3LYP cluster model calculations suggest that the favorable mode would be a μ^2-O,O′ nitrito over a short bridge Au−Au pair site. The calculated vibrational frequencies of the NO_2 adspecies are in reasonably good agreement with the experimental HREELS and IRAS spectra.

1. Introduction

The interaction of NO_2 with metal surfaces is involved in a number of commercial processes, e.g., automotive exhaust catalysis[1] and atmospheric NO_x measurement at very low concentrations.[2] So far, the adsorption and reaction of NO_2 on Pt(111),[3−6] Ru(001),[7,8] Ag(110),[9−10] Ag(111),[10−13] Pd(111),[14] Au(111),[15−18] and polycrystalline Au[19] have been investigated with a variety of experimental techniques, including TPD, LEED, EELS, HREELS, XPS, and UPS et al. While NO_2 was found to be dissociatively adsorbed on Pt(111),[3−6] Ru(001),[7,8] Ag(110),[9,10] Ag(111),[10−13] and Pd(111)[14] at rather low temperatures, molecular adsorption of NO_2 was evidenced on Au(111)[15−17] and polycrystalline Au[19] by means of TPD, HREELS, and IRAS. The desorption activation energy of NO_2 from Au(111) was estimated to be 14 kcal/mol.[15] HREELS and IRAS spectra of NO_2/Au(111) imply that at 100 K NO_2 is adsorbed on Au(111) in an O,O′ chelating form with C_{2v} symmetry.[15−17] No detailed information is available on whether the two oxygen atoms of NO_2 are bonded to one, two, or more substrate atoms.

In the present paper, the bonding of NO_2 on Au(111) has been investigated by means of quantum chemical cluster model calculations. To the best of our knowledge, this is the first electronic structure calculation dealing with the adsorption of NO_2 on metal surfaces.

It is known that in coordination compounds, NO_2 can bond with metal centers in several ways.[20] Some of these modes are depicted in Figure 1. The bonding of NO_2 with a single metal atom has been the subject of several theoretical investigations.[21−24] Previous ab initio calculations concerning $LiNO_2$ and $NaNO_2$ demonstrate that a C_{2v} bidentate structure, namely η^2-O,O′ nitrito, is the most stable.[21,22] Calculations on $[MNO_2]^+H_2O$ (M = alkaline-earth metal) are also reported.[23] Recent MP2, QCISD(T), CCSD(T), and DFT calculations predict that both $CuNO_2$ and $AgNO_2$ have a ground state of the η^2-O,O′ structure, and the bonding can be viewed as $M^+NO_2^-$ (M = Cu, Ag).[24] More recently, DFT calculations were performed to describe the ground-state reactions between NO_2 and Sc, Ti, and V, and the products were found to be OM−NO complexes.[25] So far, no previous paper has been found with regard to the $AuNO_2$ complex. The second purpose of the present work is to explore the nature of the bonding in the $AuNO_2$ molecule, comparing and contrasting $AuNO_2$ with $CuNO_2$ and $AgNO_2$, as well as the NO_2/Au(111) chemisorption systems.

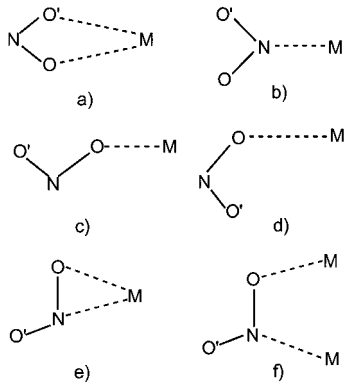

Figure 1. Some coordination modes of NO_2 to metal centers: (a) η^2-O,O′; (b) η^1-N nitro; (c) *trans*-η^1-O; (d) *cis*-η^1-O; (e) η^2-N,O; (f) μ^2-N,O.

The rest of this paper is organized as follows. In section 2, we describe the computational details. The calculated geometrical and bonding properties for the $AuNO_2$ molecule and the NO_2/Au(111) chemisorption systems are reported in subsections 3.1 and 3.2, respectively. In subsection 3.3, we present the calculated vibrational frequencies of NO_2/Au(111) and $AuNO_2$. Some concluding remarks are given in section 4.

2. Computational Details

For the $AuNO_2$ complex, five possible isomers, which are schematically presented in Figure 1a−e, have been taken into account in our calculations. These coordination modes are characterized as (a) η^2-O,O′, (b) η^1-N nitro, (c) *trans*-η^1-O, (d) *cis*-η^1-O, and (e) η^2-N,O, respectively. For NO_2 adsorption on the Au(111) surface, a 12-atom cluster model (Figure 2a) has been adopted to model the Au(111) surface. This cluster is composed of eight atoms at the first layer and four atoms at the

* Corresponding author. E-mail address: xinxu@xmu.edu.cn.

10.1021/jp9909053 CCC: $18.00
Published on Web 11/16/1999

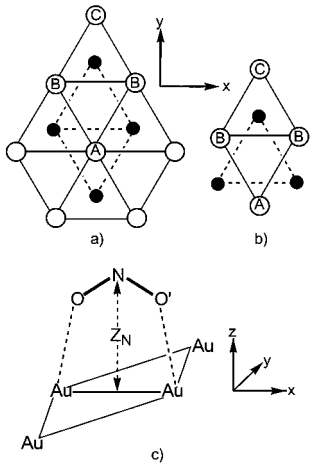

Figure 2. Cluster models of Au(111): (a) Au_{12}(8.4) (a top view); (b) Au_7(4,3) (a top view); (c) μ^2-O,O′ mode adsorption of NO_2 over a short bridge Au−Au pair site. (Open circles) Au atoms in the first layer. (Filled circles) Au atoms in the second layer.

second layer and is denoted as Au_{12}(8,4). The nearest Au−Au distance is fixed to be the bulk crystal value of 2.884 Å.[26] In this model, the on-top site (A), the short bridge site (BB), and the long bridge site (AC) are available (cf. Figure 2a). For NO_2 adsorption on top of site A, four adsorption modes were considered. These are denoted as (i) η^2-O,O′ (A1), in which NO_2 is chelated onto atom A with its two O atoms pointing to the fcc and hcp hollow sites of the Au(111) surface; (ii) η^2-O,O′ (A2), in which NO_2 is chelated onto the A atom with its two O atoms pointing to the two Au atoms that neighbor site A; (iii) η^1-N (A1), i.e., NO_2 adsorbed with N-end down onto atom A and the two O atoms pointing away from the two fcc and hcp hollow sites; and (iv) η^1-N (A2), i.e., NO_2 adsorbed with N-end down onto the A atom with its two O atoms pointing away from the two neighboring Au atoms of site A. For NO_2 chelated on the short bridge site and long bridge site, the adsorption modes are denoted as μ^2-O,O′(BB) and μ^2-O,O′(AC), respectively. A smaller cluster, Au_7(4,3) (see Figure 2b), has also been employed in the calculations of bonding energy and vibrational frequencies regarding the μ^2-O,O′ adsorption modes.

All calculations were performed with the Gaussian94 program package.[27] The hybrid density-functional B3LYP method,[28,29] which includes a mixture of Hartree−Fock exchange with DFT exchange correlation, has been employed for all the systems investigated. For $AuNO_2$, MP2 and CCSD(T) calculations have been performed for comparison. For O and N, we used the standard 6-31+G* basis sets.[27] For Au in $AuNO_2$, we used a relativistic effective core potential (RECP) to replace the 1s to 4f core electrons and treated the $5s^2$, $5p$,[6] $5d^{10}$, and $6s^1$ shells explicitly.[30] The GTO basis set for the RECP Au includes 5s, 6p, and 3d primitive functions contracted to [3s3p2d]. This basis set is referred to LanL2DZ in Gaussian94.[27] For Au in the Au_7 and Au_{12} cluster models, the smaller LanL1DZ basis set was adopted,[27] in which eight more electrons from the 5s, 5p shells are added into the RECP.

For the free NO molecule, the B3LYP calculated bond length and bond strength are 1.158 Å and 150.7 kcal/mol, in good agreement with the experimental values of 1.151 Å and 150 kcal/mol,[31] respectively. For free NO_2, the B3LYP calculated N−O bond length, O−N−O bond angle, and electron affinity (EA) are 1.202 Å, 134.0°, and 2.42 eV, while the corresponding experimental values are 1.194 Å,[32] 133.9°,[32] and 2.28 eV.[33] For the free NO_2^-, the B3LYP-calculated N−O bond length and O−N−O bond angle are 1.264 Å and 116.5°, comparable to the respective experimental values of 1.25 ± 0.02 Å and 117.5 ± 2.0°.[34]

The adsorption geometries of NO_2 were optimized in internal coordinates with the NO_2 molecular plane being perpendicular to the Au(111) surface and all the substrate atoms being fixed at the bulk geometry. Optimizations have been done by using the Berny algorithm in Gaussian94.[27] The natural bond orbital (NBO) method[35] was employed in the analysis of the bonding between NO_2 and the metal centers. For some cases, the effect of basis set superposition error (BSSE) has been examined, and corrections to the binding energies were estimated by using the counterpoise method.[36]

3. Results and Discussions

3.1. Geometric and Bonding Properties in $AuNO_2$ Complex. The optimized geometric parameters of $AuNO_2$ at the B3LYP and MP2 levels of theory are given in Table 1. We have found three local minima on the potential energy surface. These are the η^1-N nitro isomer of C_{2v} symmetry, the C_s *cis*-η^1-O nitrito isomer, and the C_s *trans*-η^1-O nitrito isomer, as demonstrated in Figure 1b,c,d, respectively. Interestingly, our MP2 and B3LYP calculations both revealed that the optimized C_{2v} η^2-O,O′ structure (cf. Table 1 and Table 7) corresponds to a transition state.

The bond dissociation energies of three isomers of $AuNO_2$ are given in Table 1. Among these isomers, the *trans*-η^1-O nitrito isomer is the least stable. The C_{2v} η^2-O,O′ structure, which is the transition state connecting the two equivalent *cis*-η^1-O isomers, is only 0.1−0.2 kcal/mol higher in energy than the *cis*-η^1-O isomer. It is difficult for B3LYP or MP2 to predict accurately the relative stability of the η^1-N and *cis*-η^1-O isomers. At the B3LYP level, the η^1-N isomer has the lowest energy, while at the MP2 level, the *cis*-η^1-O isomer becomes the most stable one. The energy difference between the two isomers is 0.5 (0.5) kcal/mol at the B3LYP level and 3.4 (2.0) kcal/mol at the MP2 level with (without) BSSE corrections. It is interesting to compare the geometric differences between the B3LYP and MP2 *cis*-η^1-O structures. We notice that the bond lengths of the two nonequivalent Au−O bonds in the MP2-derived *cis*-η^1-O structure are 2.248 and 2.257 Å, while in the B3LYP-derived *cis*-η^1-O structure they are 2.195 and 2.721 Å, respectively. As such, the MP2-derived *cis*-η^1-O structure can be regarded as a slightly distorted η^2-O,O′ structure, namely a C_s η^2-O,O′ isomer. CCSD(T) single point calculations in the B3LYP-derived and the MP2-derived geometries of these two isomers have been performed (cf. Table 1). CCSD(T) calculations are in favor of the MP2 prediction that the *cis*-η^1-O mode is by about 4.0 kcal/mol more stable than the η^1-N structure.

We then compare $AuNO_2$ with $CuNO_2$ and $AgNO_2$. Rodriguez-Santiago et al. have performed the first theoretical calculations on $CuNO_2$ and $AgNO_2$.[24] Table 2 summarizes their calculation results for MNO_2 (M = Cu, Ag) as well as ours for $AuNO_2$. On the basis of their MP2 and DFT optimization results, they found that the ground states for $CuNO_2$ and $AgNO_2$ are in the C_{2v} η^2-O,O′ structure and they predicted no *cis*-η^1-O isomers for these two molecules.[24] For $AuNO_2$, however, our MP2 and DFT calculations show that the ground state is in the *cis*-η^1-O structure; while the C_{2v} η^2-O,O′ isomer is a transition state. Our CCSD(T) calculation supports that for $AuNO_2$ the *cis*-η^1-O isomer would be somewhat more stable than the C_{2v} η^2-O,O′ isomer (cf. Tables 1 and 2). On one hand, all the calculations demonstrate that the *trans*-η^1-O isomers are considerably less stable than their corresponding ground states for all MNO_2 (M

TABLE 1: B3LYP, MP2, and CCSD(T) Calculations[a] for NO_2, NO_2^-, and $AuNO_2$

	method	Au−N /Au−O (Å)	∠AuON (deg)	O−N/N−O′ (Å)	∠ONO′ (deg)	D_e[b] (kcal/mol)	$Q(NO_2)$[g] (au)
NO_2	B3LYP			1.202	134.0		
	MP2			1.217	133.7		
	exp[c]			1.194	133.9		
NO_2^-	B3LYP			1.264	116.5		
	MP2			1.278	116.0		
	exp[d]			1.25 ± 0.02	117.5 ± 2.0		
$AuNO_2$							
η^1-N (C_{2v})	B3LYP	2.086/- - -		1.216	127.5	24.0 (22.6)	−0.29
	CCSD(T)[e]					26.8	
	MP2	2.041/- - -		1.241	125.3	19.7 (16.7)	−0.46
	CCSD(T)[f]					27.2	
cis-η^1-O (C_S)	B3LYP	- - -/2.195	107.5	1.263/1.213	119.2	23.5(22.1)	−0.40
	CCSD(T)[e]					30.3	
	MP2	- - -/2.248	100.1	1.279/1.252	115.2	21.7 (20.1)	−0.61
	CCSD(T)[f]					31.6	
trans-η^1-O (C_S)	B3LYP	- - -/2.030	113.3	1.384/1.192	109.2	11.2 (9.6)	−0.55
	MP2	- - -/2.036	108.7	1.391/1.212	110.6	12.7 (10.7)	−0.66
	CCSD(T)[f]					21.6	
η^2-O,O′ (C_{2v})	B3LYP	2.806/2.420		1.235	118.5	23.3 (22.0)	−0.40
	MP2	2.766/2.344		1.264	115.1	21.6 (20.0)	−0.62
	CCSD(T)[f]					31.5	

[a] N,O: 6-31+G*. Au: LanL2DZ. [b] $D_e = E(Au) + E(NO_2) - E(AuNO_2)$, BSSE-corrected values in parentheses. [c] Reference 32. [d] Reference 34. [e] CCSD(T) calculations by adopting the B3LYP-derived geometry. [f] CCSD(T) calculations by adopting the MP2-derived geometry. [g] Natural charge on NO_2.

TABLE 2: Relative Energies of the Different Coordination Modes of MNO_2 (M = Cu, Ag, Au) Computed with Several Methods (in kcal/mol), Dissociation Energy (D_e) of MNO_2, and the First IP of M Atoms

		coordination modes					
M	method	η^1-N	*trans*-η^1-O	*cis*-η^1-O	η^2-O,O′	D_e (kcal/mol)	first IP of M (eV)[c]
Cu[a]	DFT	5.3	11.9		0.0	45.2	(7.73)
	MP2	11.5	10.9		0.0	47.3	
	CCSD(T)	15.4	13.0		0.0	54.1	
Ag[a]	DFT	10.1	16.3		0.0	39.1	(7.58)
	MP2	12.9	13.7		0.0	37.7	
	CCSD(T)	15.6	15.0		0.0	43.9	
Au[b]	B3LYP	−0.7	12.4	−0.2	0.0	23.5	9.42 (9.23)
	MP2	1.9	8.9	−0.1	0.0	21.7	8.18
	CCSD(T)	4.3	9.9	−0.1	0.0	31.6	

[a] Computed results extracted from ref 24. [b] Present work. [c] Experimental values in parentheses.

= Cu, Ag, Au). On the other hand, the instability of the η^1-N isomers for $CuNO_2$ and $AgNO_2$ is appreciable, while the stability of the η^1-N isomer for $AuNO_2$ is comparable to its ground state. On the basis of the dissociation energies of MNO_2 listed in Table 2, we would like to conclude that the NO_2−M bonding is weaker in $AuNO_2$ than in $CuNO_2$ and $AgNO_2$, giving the following order of NO_2−M bond strength, $CuNO_2 > AgNO_2 > AuNO_2$.

NBO analyses have been performed to explore the bonding nature in the $AuNO_2$ isomers. The natural charges on the NO_2 species in these isomers are summarized in Table 1. From the data listed in Table 1, we may reach a conclusion that the charge separation between NO_2 and Au is lower at the B3LYP level than at the MP2 level, and the NO_2 unit obtains more electron charge with O coordination than that with N coordination. In general, the bonding nature in $AuNO_2$ is quite similar to that in $CuNO_2$ and $AgNO_2$.[24] Namely, there is a large electron transfer from the M (M = Cu, Ag, Au) s orbital to the singly occupied a_1 orbital of NO_2 to make an ionic $M^+-NO_2^-$ bonding in those isomers with the O coordination, and there exists a covalent interaction between the singly occupied orbitals of the neutral metal atom and NO_2 in the N coordinated structure. The feature that the geometrical parameters of the NO_2 unit in the O coordinated structures are closer to those of free NO_2^- than to those of free NO_2, while those in the N coordinated mode are more similar to those of free NO_2 than to those of free NO_2^- (cf. Table 1), provides explicit support to such a viewpoint.[24]

As far as the charge-transfer bonding characters in the nitrito complexes are concerned, it is interesting to correlate the first ionization potentials (IPs) of M (M = Cu, Ag, Au) atoms with the M−NO_2 bond strengths. For Cu and Ag, their IPs are similar and are both around 1.5 eV, smaller than that of Au (cf. Table 2). This fact would account for the similarity between $CuNO_2$ and $AgNO_2$ and the dissimilarity between $AuNO_2$ and $CuNO_2$/$AgNO_2$. The bonding in $AuNO_2$ is the weakest for its highest IP, while the $NO_2^- - M^+$ bonding is found to be stronger in $CuNO_2$ than that in $AgNO_2$ even if the first IP of Cu is somewhat higher than that of Ag.

3.2. Geometric and Bonding Properties in NO_2/Au(111) Chemisorption Systems. The Au_{12}(8,4) cluster model has a $^3A''$ ground state. NO_2 adsorption on the Au_{12} cluster model results in a $^2A''$ state for the (NO_2 + Au_{12}) systems, regardless of the adsorption modes adopted. The calculated geometric parameters and the corresponding binding energies of NO_2 adsorbed on the Au_{12}(8,4) cluster model in different modes are listed in Table 3.

In the on-top η^2-O,O′ modes and in the on-top η^1-N modes, the local geometries of the adsorbed NO_2 resemble their respective molecular analogues, i.e., the η^2-O,O′ and η^1-N isomers of $AuNO_2$, though on the Au_{12}(8,4) cluster the Au−NO_2 distances are longer than those in the $AuNO_2$ isomers. The bonding nature of NO_2/Au_{12} is similar to that in the $AuNO_2$ molecule, though the difference between modes with N coor-

TABLE 3: B3LYP Calculations[a] on the NO_2/Au_n ($n = 7, 12$) Model Systems

cluster model	adsorption mode	state	Z_N (Å)	N−O (Å)	∠ONO′(deg)	D_e[b] (kcal/mol)	$Q(NO_2)$[c]
Au_{12}	η^1-N (A1)	$^2A''$	2.451	1.244	120.8	14.0	−0.71
	η^1-N (A2)	$^2A''$	2.456	1.241	121.6	14.0	−0.69
	η^2-O,O′ (A1)	$^2A''$	3.030	1.258	116.1	22.1	−0.76
	η^2-O,O′ (A2)	$^2A''$	3.061	1.257	115.3	18.4	−0.78
	μ^2-O,O′ (AC)	$^2A''$	2.956	1.254	117.1	23.4	−0.74
	μ^2 -O,O′ (BB)	$^2A''$	3.089	1.252	119.2	28.1 (26.5)	−0.70
Au_7	μ^2-O,O′ (AC)	$^1A'$	2.894	1.247	119.1	21.8	−0.62
	μ^2-O,O′ (BB)	$^1A'$	3.030	1.244	121.2	25.5 (24.5)	−0.56
			2.920[d]	1.241[d]	123.1[d]	20.0 (17.4)[d]	−0.45[d]

[a] N,O: 6-31+G*. Au: LanL1DZ. [b] $D_e = E(NO_2) + E(Au_n) - E(NO_2/Au_n)$, BSSE-corrected values in parentheses. [c] Natural Charge on NO_2. [d] LanL2DZ basis set for Au atoms.

dination and O coordination is getting smaller, as evidenced by the calculated NBO charges on NO_2 and the bond angles ∠ONO′ listed in Table 3. The on-top η^2-O,O′ adsorptions, compared with the on-top η^1-N modes, are 5−10 kcal/mol more favorable in energy, in contrast to that observed for the $AuNO_2$ complex, in which the η^2-O,O′ and η^1-N isomers were found to have comparable stabilities by means of B3LYP calculations.

As pointed out in the Introduction, there exists a possibility that NO_2 adsorbs in a C_{2v} μ^2-O,O′ mode over the surface Au−Au pair site. Despite that no analogy of such a bonding mode has ever been found in the coordination compounds of NO_2, our calculations reveal that NO_2 adsorption in the μ^2-O,O′ mode over either the short bridge Au−Au pair site or the long bridge Au−Au site is energetically more stable than absorption in the on-top η^2-O,O′ chelating modes. NBO analyses suggest that the bonding of NO_2 adsorbed in the μ^2-O,O′ mode is quite ionic in nature and is derived by transferring one electron from the singly occupied HOMO of the Au_{12}(8,4) cluster to the singly occupied HOMO of NO_2. Thus, the NO_2 chemisorbed can be viewed as an anionic NO_2^-. Furthermore, the back-donation of charge from NO_2^- to the surface metal atoms is more feasible in the μ^2-O,O′ mode than in the on-top η^2-O,O′ mode, due to larger orbital overlap between the surface metal atoms and the NO_2^- surface species in the μ^2-O,O′ mode. As a result, the natural charge of NO_2 adsorbed in the μ^2-O,O′ mode is less negative than that in the on-top η^2-O,O′ mode (cf. Table 3).

Among all the adsorption modes considered, the μ^2-O,O′ mode over the short bridge site is the most stable. This demonstrates that for NO_2 adsorption on Au(111), the favorable adsorption geometry would be in the C_{2v} μ^2-O,O′ mode over the short bridge Au−Au pair site and supports the inference made by Koel et al. based on the HREELS[15] and IRAS[17] spectra of the NO_2/Au(111) system. It was supposed that chelating NO_2 may exist as a surface-bound radical, since the adsorbed N_2O_3 might be produced through the radical−radical types of reactions toward gas-phase NO.[15,17] Our calculations, however, found negligible net spin density on the NO_2 surface species. This finding is in agreement with the ESR observation.[18] As the adsorption bond is mainly featured with a charge transfer from the surface to NO_2, one would expect an increase in the work function of metal surface upon NO_2 chemisorption. Indeed, Koel et al. found that an increase of the work function by 1.6 eV takes place upon adsorption of a saturation coverage of chemisorbed NO_2 on Au(111).[15]

On the basis of our B3LYP calculations of the NO_2/Au_{12}-(8,4) cluster model systems, the binding energy for NO_2 adsorbed over a short bridge Au−Au pair site in the μ^2-O,O′ mode is 28.1 kcal/mol. By using the counterpoise method, a BSSE corrected binding energy of 26.5 kcal/mol is obtained. Note that the experimental activation energy for the desorption of NO_2 from the Au(111) surface given by Koel et al. is only 14 kcal/mol.[15] Therefore, the calculated binding energy is overestimated. This might be due to the shortcoming of the LanL1DZ basis set employed, as including 5s, 5p electrons into the ECP would induce inadequate description of the metal−metal bonding. For this purpose, comparative calculations have been performed on the μ^2-O,O′ (BB) NO_2/Au_7(4,3) model systems with the LanL2DZ basis set.

TABLE 4: HOMO, LUMO, IP (ionization potential), and EA (electron affinity) of the Au_n ($n = 7, 12$) Clusters Calculated at the B3LYP Level[a]

cluster	basis set	reference state	HOMO	LUMO	IP	EA
Au_{12}	LanL1DZ	$^3A''$	−4.34	−3.54	5.58	−2.32
Au_7	LanL1DZ	$^2A'$	−4.92	−4.16	6.52	−2.70
Au_7	LanL2DZ	$^2A'$	−5.73	−4.89	7.56	−3.40

[a] The work function of the Au(111) surface is 5.30 ± 0.05 eV.[37]

The calculated results for NO_2 adsorbed in the μ^2-O,O′ modes over the short bridge site (BB) as well as the long bridge site (AC) are given in Table 3. As can be seen, for the LanL1DZ basis set, the cluster size dependence of such properties as geometrical parameters and binding energies is trivial, though the cluster size does affect the amount of charge transfer from the Au cluster to NO_2. This is reasonable, as a smaller cluster should be less flexible to donate electron as compared to a larger one. For the LanL2DZ case, the calculated binding energy is 20.0 kcal/mol without BSSE correction and 17.4 kcal/mol after BSSE correction. It seems that LanL2DZ brings about a better agreement between the theoretical and experimental values.

For the cluster modeling of metal surfaces, people always encounter the dilemma that methods and basis sets of higher quality can only be applied to clusters of reduced size, while small clusters may differ considerably from the bulk solid, which makes the calculation results from small clusters less meaningful.[38−40] Table 4 tabulates the HOMO, LUMO, first IP, and EA (electron affinity) of the Au_n ($n = 7,12$) cluster models calculated at the B3LYP level. It is good to see that the (HOMO−LUMO) gaps of these clusters are all reasonably small and their HOMO levels lie within the range of −4.3 to −5.7 eV, while the Fermi level of Au(111) is −5.30 ± 0.05 eV.[37] It is well-known that the electron affinity of a conductor such as Au bulk should be equal to its electron ionization potential because its Fermi level can act as both an electron acceptor and an electron donor. This is almost impossible to obtain within the cluster models. The calculated IPs go up from Au_{12} to Au_7; EAs, however, go down as the clusters get smaller. In general, results from cluster modeling of metal surfaces should be used with caution.

3.3. Vibrational Frequencies of NO_2/Au(111) and $AuNO_2$. Table 5 presents a comparison between the experimental[41−44] and our calculated vibrational frequencies of free NO, NO_2, NO_2^-, and N_2O_3 molecules, which serves as a check for the

TABLE 5: Calculated[a,b] and Experimental Vibrational Frequencies (cm^{-1}) of NO, NO_2, NO_2^-, and N_2O_3 Molecules

	NO		NO_2		NO_2^-		N_2O_3	
Mode	B3LYP	exp[c]	B3LYP	exp[d]	B3LYP	exp[e]	B3LYP	exp[f]
$\nu(O_2N-NO)$							285	253
$\rho(O_2NNO)$							657	614
δ(ONO)			749	750	788	821	806	772
$\nu_s(NO_2)$			1398 (1328)	1325	1342 (1273)	1332	1383 (1314)	1291
$\nu_a(NO_2)$			1712 (1624)	1634	1317 (1251)	1240	1725 (1639)	1600
ν(NO)	1981 (1882)	1876					1942 (1845)	1849

[a] B3LYP/6-31+G*. [b] Scaled frequencies of the N−O stretch modes (scale factor = 0.95) in parentheses. [c] Reference 41. [d] Reference 42. [e] Reference 43. [f] Reference 44.

TABLE 6: B3LYP Calculated[a,b] and Experimental Vibrational Frequencies (cm^{-1}) of NO_2 in the NO_2/Au(111) Chemisorption Systems

	NO_2/Au_{12}			NO_2/Au_7	NO_2/Au(111)	
mode	η^1-N (A1)	η^2-O,O′ (A1)	μ^2- O,O′ (BB)	μ^2-O,O′ (BB)	HREELS[c]	IRAS[d]
$\nu(NO_2-Au)$	163	182	206	224	≥200	
rock(NO_2)	110	154	232	255		
wag(NO_2)	262	272	237	303		
δ(ONO′)	785	811	794	795	800	805
$\nu_s(NO_2)$	1352 (1284)	1304 (1239)	1295 (1230)	1277 (1213)	1180	1178
$\nu_a(NO_2)$	1431 (1359)	1286 (1221)	1337 (1270)	1386 (1317)	1180	

[a] N,O: 6-31+G*. Au: LanL1DZ. [b] Scaled values (scale factor = 0.95) in parentheses. [c] Reference 15. [d] Reference 17.

reliability of the B3LYP method to perform frequency analysis on the nitrogen oxides. It is clear that the calculated frequencies for the bending modes are in good agreement with the experimental values, while all the N−O stretching mode frequencies are overestimated. However, we found that employing a scale factor of 0.95 on all the calculated N−O stretch mode frequencies yields a better fitting to the experimental values. The scaled values are given in parentheses in Table 5. In the following paragraph, such a scaling technique will be employed in the assessment of the calculated vibrational frequencies of NO_2 in the NO_2/Au(111) chemisorption system and in the $AuNO_2$ molecule.

The calculated vibrational frequencies of NO_2 adsorption in the μ^2-O,O′(BB) mode, η^2-O,O′(A1) mode, and η^1-N(A1) mode are presented in Table 6. The experimental values extracted from HREELS[15] and IRAS[17] for the NO_2/Au(111) system are also given in Table 6.

It is easy to know that the principal normal mode vibrations for the NO_2 molecule on the metal surface in the C_{2v} O,O′ chelating mode are symmetric O−N−O′ stretch ($\nu_s(NO_2)$), asymmetric O−N−O′ stretch ($\nu_a(NO_2)$), O−N−O′ in-plane bend (δ(ONO′)), NO_2−metal stretch ($\nu(NO_2$-M)), and the rocking and wagging of NO_2. Generally speaking, only those modes with a dipole moment component normal to the surface would be observed by vibrational spectroscopy. On the basis of this surface dipole selection rule, three vibrational modes that could be observed experimentally are $\nu(NO_2-M)$, $\nu_s(NO_2)$, and δ(ONO′)). In their HREELS study[15] and the recent IRAS study[17] on the NO_2/Au(111) chemisorption system, Koel et al. observed two bands at ∼800 and ∼1180 cm^{-1}, which were tentatively ascribed to δ(ONO′) and $\nu_s(NO_2)$ vibrations of the C_{2v} O,O′ nitrito adspecies. On the basis of the off-specular scan results of HREELS experiments,[15] the O−N−O′ asymmetric stretch was assigned to be near 1180 cm^{-1}.

For NO_2 adsorption over a short bridge site in the μ^2-O,O′ mode, our calculated values of the δ(ONO′), $\nu_s(NO_2)$, and $\nu_a(NO_2)$ frequencies are 794, 1230, and 1270 cm^{-1} (scaled value). The calculated δ(ONO′), $\nu_s(NO_2)$, and $\nu_a(NO_2)$ frequencies are 811, 1239, and 1221 cm^{-1} for the η^2-O,O′(A1) mode and 785, 1284, and 1359 cm^{-1} for the η^1-N(A1) mode, respectively. It was thought that the NO_2−metal stretching mode might have a frequency of less than 200 cm^{-1}.[15] Our calculations give values of 224, 182, and 163 cm^{-1} for the NO_2−metal stretching mode in the μ^2-O,O′(BB) mode, η^2-O,O′(A1) mode, and η^1-N(A1) mode, respectively. The calculated $\nu(NO_2-Au)$ would be too low, while the calculated $\nu_s(NO_2)$ is too high in the η^1-N(A1) mode, as compared with the experimental results. The reasonable agreement of our calculated vibrational frequencies in the μ^2-O,O′(BB) mode with the experimental HREELS and IRAS spectra lends some supports to our theoretical finding that the favorable mode for NO_2 adsorption on Au(111) would be the μ^2-O,O′ nitrito over a short bridge Au−Au pair site.

TABLE 7: B3LYP-Calculated[a,b] Vibrational Frequencies (cm^{-1}) of $AuNO_2$ Complex in Different Coordination Modes

	η^1-N	*cis*-η^1-O	*trans*-η^1-O	η^2-O,O′
ω_1	250	96	142	−76
ω_2	258	272	165	235
ω_3	490	404	325	422
ω_4[c]	808	849	707vd	859
ω_5[d]	1365 (1297)	1186 (1127)	908 (863)	1315 (1249)
ω_6[e]	1632 (1550)	1543 (1466)	1683 (1599)	1460 (1387)

[a] N,O: 6-31+G*. Au: LanL2DZ. [b] Scaled values (scale factor = 0.95) in parentheses. [c] ONO′ bend mode. [d] NO symmetric stretch mode. [e] NO asymmetric stretch mode.

The calculated vibrational frequencies of the $AuNO_2$ complex in different coordination modes are given in Table 7. As pointed out in subsection 3.1, the η^2-O,O′ chelating mode possesses one imaginary frequency of −76 cm^{-1}; therefore, it is a transition state in nature. We believe that the calculated vibrational frequencies of the other three stable isomers of $AuNO_2$ should be of value in future experiments regarding this complex.

4. Concluding Remarks

Quantum chemical calculations on the bonding in the $AuNO_2$ complex have been performed at the MP2 and B3LYP levels of theory. Three isomers have been found, namely, the *trans*-η^1-O nitrito, *cis*-η^1-O nitrito, and η^1-N nitro. At the MP2 and B3LYP levels of theory, the *cis*-η^1-O nitrito and η^1-N nitro have comparable stabilities and are candidates for the ground state

of $AuNO_2$. CCSD(T) calculations prefer a ground state with the C_s η^2-O,O′ nitrito structure. The calculated binding energy for the ground state is 24.0 kcal/mol at the B3LYP level, 21.7 kcal/mol at the MP2 level, and 31.6 kcal/mol at the CCSD(T) level. The C_{2v} η^2-O,O′ nitrito structure is a transition state, which connects the two equivalent *cis*-η^1-O nitrito isomers with a low barrier height. The bonding between NO_2 and the Au atom is more ionic in the O coordinated isomers than in the N coordinated isomer.

NO_2 adsorption on Au(111) has been studied by means of hybrid B3LYP cluster model calculations. The favorable mode would be the μ^2-O,O′ nitrito over a short bridge Au−Au pair site. The adsorption is featured with electron transfer from the substrate to the adsorbate. In the present work, the best estimation of the binding energy is 17.4 kcal/mol at the B3LYP level of theory, which is in reasonable agreement with the experimental estimation of 14 kcal/mol.[15] The calculated vibrational frequencies of the μ^2-O,O′ NO_2 agree reasonably well with the experimental HREELS and IRAS spectra.[15,17]

Acknowledgment. This work was supported by the National Natural Science Foundation of China, the specific doctoral project foundation sponsored by the State Education Department of China, and Fok Ying Dung Education Foundation.

References and Notes

(1) Taylor, K. C. In *Catalysis Science and Technology*, Anderson, J. R.; Boudart, M. Eds.; Springer: Berlin, 1984; Vol. 5, p 119.
(2) Fahey, D. W.; Eubank, C. S.; Hubler, G.; Fehsenfeld, F. C. *J. Atmos. Chem.* **1985**, *3*, 435.
(3) Segner, J.; Vielhaber, W.; Ertl, G. *Isr. J. Chem.* **1982**, *22*, 375.
(4) Dahlgren, D.; Hemminger, J. C. *Surf. Sci.* **1982**, *123*, L739.
(5) Bartram, M. E.; Windham, R. G.; Koel, B. E. *Surf. Sci.* **1987**, *184*, 57.
(6) Bartram, M. E.; Windham, R. G.; Koel, B. E. *Langmuir* **1988**, *4*, 240.
(7) Schwalke, U.; Parmeter, J. E.; Weinberg, W. H. *J. Chem. Phys.* **1986**, *84*, 4036.
(8) Schwalke, U.; Parmeter, J. E.; Weinberg, W. H. *Surf. Sci.* **1986**, *178*, 625.
(9) Outka, D. A.; Madix, R. J.; Fisher, G. B.; Dimmagio, C. *Surf. Sci.* **1987**, *179*, 1.
(10) Bare, S. R.; Griffiths, K.; Lennard, W. N.; Tang, H. T. *Surf. Sci.* **1995**, *342*, 185.
(11) Polzonetti, G.; Alnot, P.; Brundle, C. R. *Surf. Sci.* **1990**, *238*, 226.
(12) Polzonetti, G.; Alnot, P.; Brundle, C. R. *Surf. Sci.* **1990**, *238*, 237.
(13) Brown, W. A.; Gardner, P.; King, D. A. *Surf. Sci.* **1995**, *330*, 41.
(14) Wickham, D. I.; Banse, B. A.; Koel, B. E. *Surf. Sci.* **1991**, *243*, 83.
(15) Bartram, M. E.; Koel, B. E. *Surf. Sci.* **1989**, *213*, 137.
(16) Wang, J.; Voss, M. R.; Busse, H.; Koel, B. E. *J. Phys. Chem. B* **1998**, *102*, 4693.
(17) Wang, J.; Koel, B. E. *J. Phys. Chem. A* **1998**, *102*, 8573.
(18) Beckendorf, M.; Katter, U. J.; Schlienz, H.; Freund, H. J. *J. Phys. C* **1993**, *5*, 5471.
(19) Wickham, D. T.; Banse, B. A.; Koel, B. E. *Catal. Lett.* **1990**, *6*, 163.
(20) Hitchman, M. A.; Rowbottom, G. L. *Coord. Chem. Rev.* **1982**, *42*, 55.
(21) Ramondo, F. *Chem. Phys. Lett.* **1989**, *156*, 346.
(22) Ramondo, F.; Bencivenni, L.; Sanna, N.; Nunziante Cesaro, S. *J. Mol. Struct. (THEOCHEM)* **1992**, *253*, 121.
(23) Rossi, V.; Sadun, C.; Bencivenni, L.; Caminiti, R. *J. Mol. Struct. (THEOCHEM)* **1994**, *314*, 247.
(24) Rodriguez-Santiago, L.; Branchadell, V.; Sodupe, M. *J. Chem. Phys.* **1995**, *103*, 9738.
(25) Stirling, A. *Chem. Phys. Lett.* **1998**, *298*, 101.
(26) *Handbook of Chemistry and Physics*; CRC Press: Cleverland, OH, 1984−1985.
(27) Frisch, M. J.; Trucks, G. W.; Schlegel, H. B.; Gill, P. M. W.; Johnson, B. G.; Robb, M. A.; Cheeseman, J. R.; Keith, T.; Petersson, G. A.; Montgomery, J. A.; Raghavachari, K.; Al-Laham, M. A.; Zakrzewski, V. G.; Ortiz, J. V.; Foresman, J. B.; Peng, C. Y.; Ayala, P. Y.; Chen, W.; Wong, M. W.; Andres, J. L.; Replogle, E. S.; Gomperts, R.; Martin, R. L.; Fox, D. J.; Binkley, J. S.; Defrees, D. J.; Baker, J.; Stewart, J. P.; Head-Gordon, M.; Gonzalez, C.; Pople, J. A. *Gaussian 94*; Gaussian, Inc.: Pittsburgh, PA, 1995.
(28) Becke, A. D. *J. Chem. Phys.* **1993**, *98*, 5648.
(29) Lee C.; Yang, W.; Parr, R. G. *Phys. Rev. B* **1988**, *37*, 785.
(30) Hay, P. J.; Wadt, W. R. *J. Chem. Phys.* **1985**, *82*, 299.
(31) Herzberg, G. *Electronic Spectra of Polyatomic Molecules*; Van Nostrand Reinhold: New York, 1966.
(32) Morino, Y.; Tawimoto, M.; Saito, S.; Hirota, E.; Awata, R.; Tanaka, T. *J. Mol. Spectrosc.* **1983**, *98*, 331.
(33) Hughes, B. M.; Lifschitz, C.; Tienan, T. O. *J. Chem. Phys.* **1973**, *59*, 3162.
(34) Ervin, K. M.; Ho, J.; Lineberger, W. C. *J. Chem. Phys.* **1988**, *92*, 5404.
(35) Carpenter, J. E.; Weinhold, F. *J. Mol. Struct. (THEOCHEM)* **1988**, *169*, 41.
(36) Boys, S. F.; Bernard, F. *Mol. Phys.* **1970**, *19*, 553.
(37) Lecoeur, J.; Bellier, J. P.; Koehler, C. *Electrochim. Acta* **1990**, *35*, 1383.
(38) Panas, I.; Schüe, J.; Siegbahn, P.; Wahlgren, U. *Chem. Phys. Lett.* **1988**, *149*, 265.
(39) Xu, X.; Wang, N.; Lu, X.; Chen, M.; Zhang, Q. *Sci. Chin. B* **1995**, *38*, 1038.
(40) Xu, X.; Wang, N.; Zhang, Q. *Bull. Chem. Soc. Jpn.* **1996**, *69*, 529.
(41) Herzberg, G. *Spectra of Diatomic Molecules*; Molecular Spectra and Molecular Structure, Vol. 1; Van Nostrand-Reinhold: New York, 1945.
(42) Lafferty, W. J.; Sams, R. L. *J. Mol. Spectrosc.* **1977**, *66*, 478.
(43) Watson, R. E.; Brodasky, T. F. *J. Chem. Phys.* **1957**, *27*, 683.
(44) Hisatsune, I. C.; Devlin, J. P. *Spectrochim. Acta* **1960**, *16*, 401.